Abdominal Radiology (2020) 45:3155–3162
https://doi.org/10.1007/s00261-019-02372-x

PANCREAS

Pancreatic neuroendocrine tumors (pNETs): the predictive value of MDCT characteristics in the differentiation of histopathological grades

Faeze Salahshour[1] · Mohammad-Mehdi Mehrabinejad[1,3] · Ali Zare Dehnavi[1,3] · Abbas Alibakhshi[2] · Habibollah Dashti[2] · Mohammad-Ali Ataee[1] · Niloofar Ayoobi Yazdi[1]

Published online: 2 January 2020

Abstract

Purpose To investigate the correlation between multiple detector computed tomography (MDCT) features of pancreatic neuroendocrine tumors (pNETs) and histopathologic grade and find valuable imaging criteria for grade prediction.

Material and methods MDCT of 61 patients with 65 masses, which pNETs were approved histopathologically, underwent revision retrospectively. Each MDCT was evaluated for various radiologic characteristics. Absolute and relative (*R*: tumor/pancreas, *D*: tumor–pancreas) tumor enhancements were calculated in multiple post contrast phases.

Results 61 patients [mean age = 50.70 ± 14.28 y/o and 30(49.2%) were male] were evaluated and classified into 2 groups histopathologically: G_1: 32 (49.2%) and $G_{2,3}$: 33 (50.8%). Significant relationships were observed between histopathologic tumor grade regarding age ($p = 0.006$), the longest tumor size ($p = 0.006$), presence of heterogeneity ($p < 0.0001$), hypodense foci in delayed phase ($p = 0.004$), lobulation ($p = 0.002$), vascular encasement ($p < 0.0001$), adjacent organ invasion ($p = 0.01$), presence ($p < 0.0001$) and number (0.02) of liver metastases, presence of lymphadenopathy with short axis of more than 10 mm (LAP) ($p = 0.008$), pathologic lymph node size ($p = 0.004$), relative (R and D) ($p = 0.05$ and 0.02, respectively), and percentage of arterial hyper-enhancing area ($p = <0.0001$). Tumor grades, however, had no significant relationship with gender, tumor location, tumor outline, calcification, cystic change, or pancreatic (PD) or biliary duct (BD) dilation ($p = 0.21$, 0.60, 0.05, 0.05 1, 0.10, and 0.51, respectively). Then, we suggested a novel imaging criteria consisting of six parameters (tumor size > 33 mm, relative (R) tumor enhancement in arterial phase ≤ 1.33, relative (D) tumor enhancement in arterial phase ≤ 16.5, percentage of arterial hyper-enhancing area ≤ 75%, vascular encasement, and lobulation), which specificity and accuracy of combination of all findings (6/6) for predicting $G_{2,3}$ were 100% and 70.1%, respectively. The highest accuracy (84.21%) was seen in combinations of at least 4 of 6 findings, with 80.00% sensitivity, 87.5% specificity, 83.33% PPV, and 84.85% NPV.

Conclusion We suggested reliable imaging criteria with high specificity and accuracy for predicting the histopathologic grade of pNETs.

Keywords Pancreatic neuroendocrine tumors · Multidetector computed tomography · Pathologic grade

✉ Niloofar Ayoobi Yazdi
nayoobi@sina.tums.ac.ir

[1] Department of Radiology, School of Medicine, Advanced Diagnostic and Interventional Radiology Research Center (ADIR), Imam Khomeini Hospital, Tehran University of Medical Sciences, Tehran 1419733141, Iran

[2] Hepatobiliary and Liver Transplantation Division, Department of General Surgery, Imam-Khomeini Hospital, Tehran University of Medical Sciences (TUMS), Tehran, Iran

[3] Students Scientific Research Center, Tehran University of Medical Sciences, Tehran, Iran

Introduction

Pancreatic neuroendocrine tumors (pNETs) are rare tumors that originate from the neuroendocrine cells of the pancreas [1]. They account for less than 3% of pancreatic tumors, with an annual incidence of one case per 100,000 individuals per year [1, 2]. Nevertheless, pNETs are considered to be potentially malignant neoplasms [3].

pNETs are categorized into functioning (F-pNETs) and non-functioning (NF-pNETs) based on the existence of clinical symptoms due to hormone hypersecretion [2], and they

are histopathologically classified into three types of neuroendocrine tumors known as grade 1 (G_1) and grade 2 (G_2), and neuroendocrine carcinomas grade 3 (G_3) according to the World Health Organization (WHO) 2010 classification. This grading is based on the mitotic rate and Ki-67 index and indicates the malignant potential of these tumors [4]. The histological grade of a pNET is meaningfully associated with the prognosis and long term survival of the patient [1] and represents the malignant nature of the tumor; thus, it has considerable impact on therapeutic protocols [5]. Surgery is still considered as the treatment of choice for localized pNETs and results in a considerably higher survival rate [1].

Computed tomography (CT) is the key modality for assessing pNETs because of its high resolution [3]. The incidence of pNETs has increasingly been reported in recent decades by means of incidental finding through imaging procedures. This has led to a growing number of questions concerning treatment approaches [1, 5]. Despite several surveys that have studied the imaging features in pNETs and revealed the predictive capability of CT scan in differentiating the histopathologic grade of pNETs [4, 6–9], just limited studies have suggested MDCT-based criteria [1, 5] and there is no common consensus regarding reliable imaging criteria for pNETs grades prediction [3].

The objectives of the current study were to evaluate the features of Multiple Detector Computed Tomography (MDCT) to prognosticate the histopathological grade of pNETs: size, location, heterogeneity, hypodense foci in the delayed phase, and absolute and relative tumor enhancement, to name but a few, and to suggest novel imaging criteria to trustworthily predict tumor grades.

Materials and methods

Study design and patients

This retrospective study was reviewed and approved by our Institutional Review Board. All patients who underwent surgical resection of pNETs between 2014 and 2018 were evaluated. All participants had an MDCT within at least 30 days before surgery and a histological pathology report. All patients with a non-visible mass on pre-operative MDCT or pre-operative local treatment or chemotherapy were excluded. Age, gender, and surgery type were obtained from the institutional database. A total of 61 patients with 65 masses (two patients had three masses) were included in the current survey, of whom 32 (49.2%) were male. Patients ranged in age from 16 to 77.

Histopathological analysis

All operative specimens were evaluated by one expert pathologist and were classified according to the 2010 WHO guidelines [10]. Classification was based on the mitotic rate per 10 high-power fields (HPF) and the Ki-67 index in immunohistochemistry as: G_1: mitotic count < 2 per 10 HPF; Ki-67 ≤ 3%; G_2 (well differentiated): mitotic count 2–20 per 10 HPF; Ki-67 3-20%; and G_3 (poorly differentiated): mitotic count > 20 per 10 HPF; Ki-67 > 20%. In non-concordance between the mitotic rate and the Ki-67 index, the higher grade was considered. In addition to grading, tumor size and presence of necrosis in the lesions were reported. As the histopathology of our population study lesions was reported between 2014 and 2018, the pathologist used the latest version of WHO neuroendocrine neoplasm (NEN) classification, which was the 2010 edition at that time. The main difference between 2010 and 2017 WHO grading system is about G_3 tumors. In the 2010 version, grading was only based on the ki-67 index, and mitoses/10 HPF and lesions with ki-67 > 20 and/or mitoses/10HPF > 20 were placed in the G_3 group. However, in the 2017 version, lesions with the above-mentioned ki-67 figures are categorized into two subgroups based on their morphology: well differentiated (NET grade 3) and poorly differentiated (NEC grade 3) [11]. As our study only consists of 5 (7.7%) grade 3 lesions, which were merged to the G_2 group, it seems that the distinction of these five cases by the new version will not cause a significant change in the results of the study.

MDCT imaging technique

All CT scan examinations were carried out on either the Lightspeed 64-detector CT)GE Healthcare, Milwaukee, USA(or the Siemens SOMATOM Emotion (16 slices, Erlangen, Germany(MDCT scanner. The imaging parameters for both non-contrast and contrast-enhanced phases were 2–3 mm section thickness; beam collimation of 0.6–2 mm; 120 kVp tube voltage; tube current, 150–250 mAs; tube rotation speed of 0.75 seconds; and gantry rotation times, 0.5–0.75 s. Dynamic CT images, including non-contrast, arterial, portal venous, and delayed phase imaging (at 0, 22–40, 52–70, and 180 seconds, respectively), were performed for 53(86.8%) patients (57 (87.6%) tumors), and the remaining 8 (13.1%) patients (8 (12.3%) pNETs) had less than four but at least one contrast-enhanced phase MDCT. Following the non-contrast imaging, non-ionic iodinated contrast (80–100 ml of Omnipaque (Daiichi Sankyo, Tokyo, Japan)) with a concentration of 350 mg/ml and the speed rate

of 4 ml/s, followed by 30-40 ml saline flush was injected into peripheral veins.

Image analysis

Two radiologists with 8 and 12 years of experience in abdominal radiology and blinded to pathology reports independently evaluated MDCT features. Imaging features were divided into the two categories of qualitative and quantitative. Qualitative features included (1) tumor location: head, uncinate process, neck, body, tail, and multifocal or diffuse; (2) homogeneity or heterogeneity; (3) cystic change: defined as non-enhancing ovoid or circular lesions with well-delineated margins; (4) lobulation: multiple small rounded outpouchings extending from the tumor border; (5) ill-defined hypodense foci in delayed phase; (6) tumor outline: well-defined or ill-defined border; (7) presence of pancreatic (PD) or biliary (BD) duct dilation: PD, intrahepatic and extra hepatic BD dilation were defined as >3 mm, >2 mm, and >8 mm, respectively; (8) existence of liver metastasis; (9) invasion of adjacent organs; (10) lymphadenopathy (LAP): lymph nodes with a short axis diameter of more than 10 mm; (11) vascular encasement; (12) phase of peak enhancement: arterial, portal, and delayed phase; and (13) calcification: evaluated by non-contrast MDCT.

Quantitative tumor features consisted of (1) tumor size: the longest diameter in different planes; (2) tumor attenuation [based on Hounsfield units (HU)]: by placing a 10 mm region of interest (ROI) and carefully avoiding calcified, cystic, or necrotic areas, PD, and vessels; (3) number of liver metastases; (4) percentage of arterial hyper-enhanced area in the tumor; (5) pathologic lymph node size: size of short axis diameter (mm) was recorded if was more than 10 mm; (6) absolute tumor enhancement: defined as the difference of the attenuation of the tumor in any phases with non-enhancing phase; (7) relative (Ratio (R)) tumor enhancement: calculated by dividing the tumor attenuation by normal pancreas attenuation in different MDCT phases; and (8) relative (difference (D)) tumor enhancement: defined as the difference of the attenuation of the tumor with normal pancreas in different MDCT phases.

To evaluate the intra-rater reliability, each radiologist reviewed some cases two weeks later anonymously and Intraclass Correlation Coefficient (ICC) was measured. If ICC ≥ 0.8, we would recorded the lower measurement, and if ICC <0.8, we recorded the mean of two measurements.

To assess the Inter-rater reliability, the values recorded by two radiologists were observed, and the Intraclass Correlation Coefficient (ICC) was measured. In case of ICC <0.8, any non-concurrence in image interpretation between them was resolved by consensus. If ICC ≥ 0.8, the value recorded by the radiologist with more experience was used.

All variables were examined in all 65 pNETs, but tumor enhancement rates (absolute and relatives) were assessed in 57 pNETs who had triphasic MDCT. Hypodense foci were evaluated in 61 pNETs that had delayed phase MDCT.

Ethics

This study was carried out in accordance with the World Medical Association Declaration of Helsinki and approved by the Ethics Committee of our institute. After the goals of the study were explained to them, participants signed consent forms and were assured that their individual data would remain confidential to the research team.

Statistical analysis

Data analysis was performed using IBM SPSS 16 for Windows (Chicago, IL, USA). A p-value <0.05 was considered statistically significant. Descriptive data (minimum, maximum, range, mean, and standard deviation) of all variables were calculated for all participants. Absolute and relative tumor enhancements were computed by SPSS. The chi-square and Fisher's exact tests were performed to determine the relationship between qualitative variables. Kolmogorov–Smirnov test were performed to determine the normality distribution of data. The Mann–Whitney U test, a non-parametric test, was used to assess the relationship between quantitative variables and tumor grades. To define the optimum cut-off values for the most significant MDCT finding in the differentiation of tumor grades, the Receiver Operating Characteristic (ROC) curves were drawn and Youden's index [12] was used. Logistic regression (backward) was performed to find a model with higher accuracy. The sensitivity, specificity, Positive Predictive Value (PPV), Negative Predictive Value (NPV), and accuracy for the differentiation between tumor grades were calculated for each parameter and for combinations of 2 or 3 of them.

Results

The mean patient age was 50.70 ± 14.28 years (ranging from 16 to 77), and 30 (49.2%) participants were male. Mean tumor size was 47.52 ± 39.4 mm. Two patients had three pNETs. Histopathologic analysis showed that 32 of 65 pNETs (49.2%) were confirmed to be G_1 pNETs, 28 (43.1%) were G_2 pNETs, and 5 (7.7%) were G_3 pNETs. G_2 and G_3 were combined into a single group ($G_{2,3}$: 33 (50.8%)) due to small quantity (Table 1).

Of 65 pNETs, 25 (38.5%) were in the head or uncinate process of the pancreas, 4 (6.2%) were in the neck, 11 (16.9%) were in the body, 18 (27.7%) were in the tail, 4 (6.2%) were in the body and tail, 2 (3.1%) were diffuse, and

Table 1 Qualitative MDCT features in different histopathological grades of pNETs

Variables	Grade		
	1	2,3	*p*-value
	n (%)		
Number	32 (49.2)	33 (50.8)	
Sex			
Male	13 (40.6)	19 (59.4)	0.21
Female	19 (57.6)	14 (42.4)	
Homogeneity			
Homogeneous	14 (93.3)	1 (6.7)	<0.0001*
Heterogeneous	18 (36.0)	32 (64.0)	
Liver metastasis			
Yes	0 (0)	11 (100)	<0.0001*
No	32 (59.3)	22 (40.7)	
LAP			
Yes	3 (18.8)	13 (81.3)	0.008*
No	29 (59.2)	20 (40.8)	
Hypodense foci in delayed phase			
Yes	3 (17.6)	14 (82.4)	0.004*
No	27 (61.4)	17 (38.6)	
Adjacent organ invasion			
Yes	0 (0)	7 (100)	0.01*
No	32 (55.2)	26 (44.8)	
Vascular encasement			
Yes	0 (0)	14 (100)	<0.0001*
No	32 (62.7)	19 (37.3)	
Lobulation			
Yes	14 (34.1)	27 (65.9)	0.002*
No	18 (75.0)	6 (25.0)	
Tumor outline			
Ill-defined	0 (0)	5 (100)	0.05
Well-defined	32 (53.3)	28 (46.7)	
PD dilation			
Yes	3 (25.0)	9 (75.0)	0.10
No	29 (54.7)	24 (45.3)	
BD dilation			
Yes	4 (36.4)	7 (63.6)	0.51
No	28 (51.9)	26 (48.1)	
Cystic change			
Yes	8 (47.1)	9 (52.9)	1
No	24 (50.0)	24 (50.0)	
Calcification			
Yes	13 (68.4)	6 (31.6)	0.05
No	19 (41.3)	27 (58.7)	

PD pancreatic duct, *BD* biliary duct, *LAP* lymphadenopathy
*Statistically significant

1 (1.5%) was in head, uncinated process, neck, and proximal body. Whipple surgery and enucleation were the most prevalent surgical methods ([3] 29.5% for both).

Fig. 1 The pre-operative MDCT of a 67 year-old man with G3 pNET and necrosis in pathology after distal pancreatectomy. Arrows: Hypodense foci is seen in delayed phase

Both ICC values (for inter- and intra-rater reliability) were > 0.8. A significant association was observed between hypodense foci in the delayed phase on radiologic imaging and necrosis in histopathology ($p = 0.004$) (Fig. 1).

Data analysis illustrated the significant relationships between histopathologic tumor grade with respect to age ($p = 0.006$), the longest tumor size ($p = 0.006$), presence of heterogeneity ($p < 0.0001$), hypodense foci in delayed phase ($p = 0.004$), lobulation ($p = 0.002$), vascular encasement ($p < 0.0001$), adjacent organ invasion ($p = 0.01$), presence and number of liver metastases ($p < 0.0001$ and 0.02, respectively), LAP ($p = 0.008$), and lymph node size ($p = 0.004$) (Tables 2, 3). All patients with one of the following features were in $G_{2,3}$: liver metastasis (Fig. 2), adjacent organ invasion, vascular encasement, and ill-defined border (Table 1).

Tumor grades, however, had no significant relationship with gender, tumor location, cystic change, or PD or BD dilation ($p = 0.21$, 0.60, 1, 0.10, and 0.51, respectively) (Table 1). Meanwhile, this association was marginally significant for tumor outline ($p = 0.05$) and calcification ($p = 0.05$) (Table 1).

Further analysis revealed that lower relative (*R*) tumor enhancement in delayed phase ($p = 0.03$) and relative (*D*) tumor enhancement in arterial and delayed phases ($p = 0.02$ and 0.02, respectively) were significantly correlated with higher histopathologic grade (Fig. 3); absolute tumor attenuation, however, was higher in G_1 in arterial, portal venous, and delayed phase but did not show a significant difference ($p = 0.63$, 0.53, and 0.05, respectively) (Table 2). In addition, it was determined that the lower peak of absolute tumor enhancement (HU) was marginally associated with higher grade ($p = 0.05$), and a lower percentage of arterial

Table 2 Quantitative MDCT features in different histopathological grades of pNETs

Variables	Grade		*p*-value
	1	2,3	
	Mean (SD)		
Age	54.3 (13.4)	44.27 (14.9)	0.006*
Tumor size	34.3 (39.5)	60.3 (34.4)	0.006*
Lymph node size	1.0 (3.2)	8.1 (12.7)	0.004*
Number of liver metastases	0 (0)	4.6 (11.3)	0.02*
Relative (*R*) tumor enhancement			
Arterial	1.27 (0.36)	1.23 (0.74)	0.05
Portal	1.21 (0.31)	1.22 (0.54)	0.25
Delayed	1.25 (0.24)	1.17 (0.44)	0.03*
Relative (*D*) tumor enhancement			
Arterial	25.57 (27.42)	11.79 (34.86)	0.02*
Portal	17.91 (26.26)	12.76 (24.20)	0.21
Delayed	18.00 (17.32)	7.04 (15.29)	0.02*
Absolute tumor enhancement			
Arterial	73.28 (37.52)	65.56 (33.88)	0.63
Portal	76.31 (70.82)	70.83 (26.00)	0.53
Delayed	49.18 (17.79)	38.15 (17.63)	0.05
Peak of absolute tumor enhancement	132.18 (35.84)	114 (32.20)	0.05
Percentage of arterial hyper-enhancing area in the tumor	90.5 (41.2)	44.7 (34.7)	< 0.0001*

R ratio (tumor/pancreas), *D* difference (tumor–pancreas)

*Statistically significant

Table 3 Sensitivity, specificity, PPV, NPV, and accuracy of MDCT findings for predicting the G2,3 of pNETs

MDCT findings	Sensitivity	Specificity	PPV	NPV	Accuracy
Size > 33 mm	84.00	71.88	70.00	85.19	77.19
Relative (*R*) tumor enhancement ≤ 1.33 (in arterial phase)	80.00	53.12	57.14	77.27	64.91
Relative (*D*) tumor enhancement ≤ 16.5 (in arterial phase)	64.00	75.00	66.67	72.73	70.18
Percentage of arterial hyper-enhancing area ≤ 75%	84.00	75.00	72.41	85.71	78.95
Vascular encasement	52.00	100	100	72.73	78.95
Lobulation	88.00	56.25	61.11	85.71	70.18
≥ 3 of 6	88.00	68.75	68.75	88.00	77.19
≥ 4 of 6	80.00	87.50	83.33	84.85	84.21
≥ 5 of 6	52.00	90.62	81.25	70.73	73.68
6 of 6	32.00	100	100	65.31	70.18

PPV positive predictive value, *NPV* negative predictive value

hyper-enhancing area in the tumor was correlated with a higher grade ($p < 0.0001$) (Table 2).

In logistic regression among all related variables the following imaging feature remained significant in the model after adjusting for confounders. We used 33 mm for tumor size (area under ROC curve = 0.824, $p < 0.0001$, 95% CI 0.712–0.935, Youden's index: 0.559), 1.33 for relative (*R*) tumor enhancement in the arterial phase (area under ROC curve: 0.657, $p = 0.04$, 95% CI 0.503–0.811, Youden's index: 0.319), 16.5 for relative (*D*) tumor enhancement in the arterial phase (area under ROC curve: 0.679, $p = 0.02$, 95% CI 0.529–0.829, Youden's index: 0.370), and 75% for percentage of arterial hyper-enhancing area (area under ROC curve: 0.847, $p < 0.001$, 95% CI 0.724–0.969, Youden's index: 0.644) as cut-off values, and the following findings were assessed to predict $G_{2,3}$: size > 33 mm, relative (*R*) tumor enhancement ≤ 1.33, relative (*D*) tumor enhancement ≤ 16.5, percentage of arterial hyper-enhancing area ≤ 75%, vascular encasement, and lobulation (Fig. 3). Sensitivity, specificity, PPV,

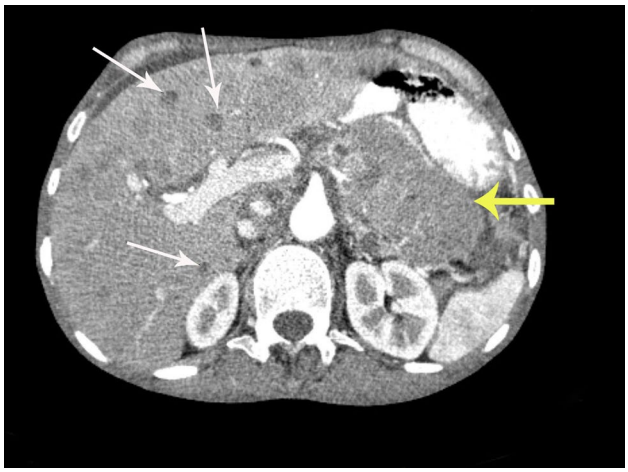

Fig. 2 A 55 year-old man with 90 mm pNET in body and tail of the pancreas (yellow arrow), with multiple metastatic lesions in liver (white arrows). pNET grade was reported G3 in histopathologic investigations

NPV, and accuracy were calculated for each parameter and combinations of 3, 4, 5, or 6 of them are illustrated in Table 3. The combination of 6 findings, surprisingly, had the highest (100%) specificity and PPV, but 32.0% and 70.18% sensitivity and accuracy, respectively. The highest accuracy (84.21%) was seen in combinations of at least 4 of 6 findings, with 80.00%, 87.5%, 83.33%, and 84.85% sensitivity, specificity, PPV, and NPV, respectively.

Discussion

Despite their low incidence, pNETs have been increasingly reported over the last few decades. The prognosis and treatment of pNETs are significantly dependent upon tumor grade, and just limited previous studies have suggested imaging criteria for predicting tumor grade [1, 5]. To specify the appropriate treatment for pNETs, it is shown that WHO 2010 grading system can be used as reliable mean for predicting survival rate and lesions ≤ 2 cm which are mostly G1 pNETs can be managed conservatively by non-surgical approaches [13, 14]. These lesions can be follow upped by serial radiologic studies [15]. The current study aimed to introduce MDCT features that could significantly estimate pNET grading and help clinicians choose the most appropriate treatment approach.

In the current survey, 50.8% of pNETs were $G_{2,3}$, and the rest were G_1. Previous studies have also reported the same proportion [1, 3, 5]. It is noteworthy to point that inter- and intra-rater reliability was high enough using ICC, indicating high value of further interpretations.

The current study suggests the following MDCT features as the major predictors of $G_{2,3}$: tumor size, heterogeneity, hypodense foci in delayed phase, liver metastasis, LAP, lymph node size, adjacent organ invasion, lobulation, vascular encasement, relative (*R*) tumor enhancement in delayed phase, relative (*D*) tumor enhancement in arterial and delayed phase, and percentage of arterial hyperenhancing area in the tumor. All the pNETs who had just one of the following imaging features showed $G_{2,3}$: liver metastasis, adjacent organ invasion, vascular encasement, and ill-defined border.

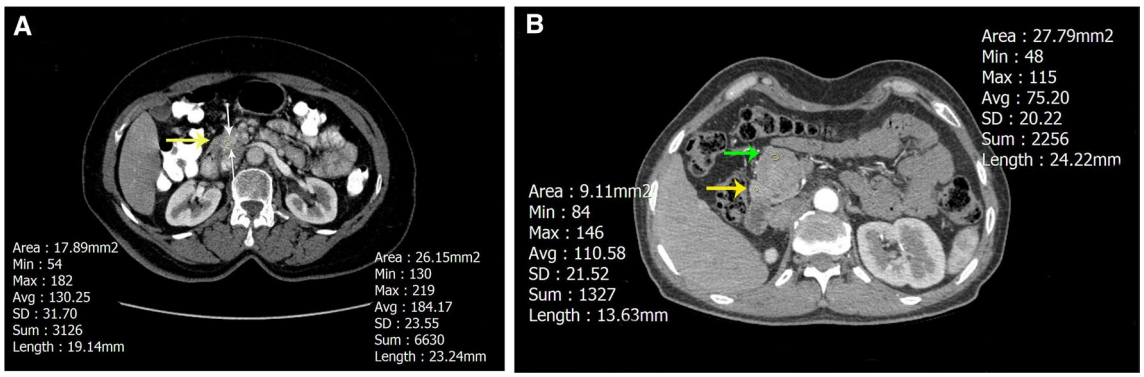

Fig. 3 Examples of the predictive value of the MDCT for pNET grades. **a** A 69 year-old woman with 15 mm pNET in head of pancreas (white arrows) and normal pancreas (yellow arrow). Relative (R) tumor enhancement = 1.41 (> 1.33) and relative (D) tumor enhancement = 53.8 (> 16.5) suggestive for lower grade that is compatible with histopathologic examination (G1). **b** A 54 year-old man with 40 mm pNET in neck of the pancreas (green arrow) and normal pancreas (yellow arrow). Relative (R) tumor enhancement = 0.68 (< 1.33) and relative (D) tumor enhancement = − 35.3 (< 16.5) suggestive for higher grades that is compatible with histopathologic evaluation (G2)

This association was marginally significant for calcification and tumor outline. Another novel finding of this study is the noteworthy connection between hypodense foci in MDCT and necrosis in the histopathology report.

In line with the current findings, Luo et al. reported tumor size, metastasis, LAP, and adjacent organ invasion as valuable predictors of the higher histopathological grade of pNETs, but inconsistent with the current study, ill-defined border tumors and PD dilation were also reported higher in G_2 pNETs [4]. Similar to the current results, several studies reported that calcification was not significantly associated with tumor grade [1, 3, 6]. Discrepancy is noticeable among various studies in terms of reliable predictability of tumor outline, PD dilation, and cystic change for histopathologic grading [1, 4, 6, 7]. Worhunsky et al. reported the same relationship between hypodense foci and necrosis in histopathology [16].

Notably that in recent years, the analysis methods of medical images have progressed rapidly. One tool which eased the way for analysis radiologic data by conversion of images into a good source of quantitative information is named radiomics, and specifically for CT, it is called CT Texture Analysis (CTTA) [3]. Few studies have revealed that this method can be applied for prediction of PNET grading or even their post-surgical flare up and as a result, facilitate the management of PNET cases [17, 18]. However, in a study by Tae Won Choi et al. in which CTTA using 3D arterial phase was relatively more accurate than CT features; however, their findings did not show a significant difference between these two methods [3].

Analysis in the current study illustrated that relative (*R* and *D*) tumor enhancement ratios and percentage of arterial hyper-enhancing area in the tumor were conversely correlated with tumor grade. These were also investigated in several studies and showed a considerable difference between two histopathologically-based categories [1, 6].

The current study suggests novel imaging criteria with 100% specificity and PPV in forecasting $G_{2,3}$ tumors, comprising tumor size > 33 mm, relative (R) tumor enhancement ≤ 1.33 (in arterial phase), relative (*D*) tumor enhancement ≤ 16.5 (in arterial phase), percentage of arterial hyper-enhancing area ≤ 75%, vascular encasement and lobulation; combinations of at least 4 of 6 of them showed the highest accuracy (84.21%) and 80.00% sensitivity, 87.5% specificity, 83.33% PPV, and 84.85% NPV in predicting the higher grades and is recommended to be applied in clinical settings. Combinations of at least 6 of 6 imaging features had the 100% specificity and PPV as well as 70.1% accuracy in estimating the higher histopathological grades. Limited parallel studies have recommended different criteria, among which tumor size and tumor enhancement are the only mutual parts. These surveys, however, had lower specificity and accuracy compared with the current study [1, 5, 19].

The findings of the current study have to be seen in light of some limitations. The first is selection bias due to retrospective design of the study. Furthermore, our study included a relative small study population and particularly we had only 5 G_3 pNET lesions, therefore, further multicentric investigations are required to approve our findings. Another limitation is exclusion of all cases with no visible lesion on pre-operative MDCT. At last, as biopsy may not reliably diagnose *G3* lesions, patients limited to those who underwent surgical resection.

Conclusion

Some MDCT features were found in this study which help in the differentiation between G_1 and $G_{2,3}$ pNETs. A tumor size > 33 mm, relative (*R*) tumor enhancement < 1.33 (in arterial phase), relative (*D*) tumor enhancement ≤ 16.5 (in arterial phase), percentage of arterial hyper-enhancing area ≤ 75%, vascular encasement and lobulation could significantly predict $G_{2,3}$. Accordingly, we suggested reliable imaging criteria with great specificity, PPV and accuracy to provide clinicians with a better estimation for planning therapeutic approaches. This notion require further surveys on larger population to be confirmed.

Acknowledgements The authors are thankful to the patients and Imam Khomeini hospital staff for their collaboration.

Compliance with ethical standards

Conflict of interest The authors of this manuscript declare conflicts of interest.

References

1. Belousova E, Karmazanovsky G, Kriger A, Kalinin D, Mannelli L, Glotov A, et al. Contrast-enhanced MDCT in patients with pancreatic neuroendocrine tumours: correlation with histological findings and diagnostic performance in differentiation between tumour grades. Clin Radiol [Internet]. 2017 Feb [cited 2019 May 20];72(2):150. Available from: http://www.ncbi.nlm.nih.gov/pubmed/27890421
2. Paiella S, Impellizzeri H, Zanolin E, Marchegiani G, Miotto M, Malpaga A, et al. Comparison of imaging-based and pathological dimensions in pancreatic neuroendocrine tumors. World J Gastroenterol [Internet]. 2017 May 7 [cited 2019 May 23];23(17):3092–8. Available from: http://www.ncbi.nlm.nih.gov/pubmed/28533666
3. Choi TW, Kim JH, Yu MH, Park SJ, Han JK. Pancreatic neuroendocrine tumor: prediction of the tumor grade using CT findings and computerized texture analysis. Acta radiol [Internet]. 2018 Apr 2 [cited 2019 May 23];59(4):383–92. Available from: http://www.ncbi.nlm.nih.gov/pubmed/28766979
4. Luo Y, Dong Z, Chen J, Chan T, Lin Y, Chen M, et al. Pancreatic neuroendocrine tumours: correlation between MSCT features and pathological classification. Eur Radiol [Internet]. 2014 Nov 22

[cited 2019 May 20];24(11):2945–52. Available from: http://link.springer.com/10.1007/s00330-014-3317-4
5. Kim DW, Kim HJ, Kim KW, Byun JH, Song KB, Kim JH, et al. Neuroendocrine neoplasms of the pancreas at dynamic enhanced CT: comparison between grade 3 neuroendocrine carcinoma and grade 1/2 neuroendocrine tumour. Eur Radiol [Internet]. 2015 May 3 [cited 2019 May 20];25(5):1375–83. Available from: http://link.springer.com/10.1007/s00330-014-3532-z
6. Hyodo R, Suzuki K, Ogawa H, Komada T, Naganawa S. imaging findings and pathological grading.Pancreaatic neuroendocrine tumors containing areas of iso- or hypoattenuation in dynamic contrast-enhanced computed tomography: Spectrum of. Eur J Radiol [Internet]. 2015 Nov [cited 2019 May 20];84(11):2103–9. Available from: http://www.ncbi.nlm.nih.gov/pubmed/26321494
7. Rodallec M, Vilgrain V, Couvelard A, Rufat P, O'Toole D, Barrau V, et al. Endocrine pancreatic tumours and helical CT: Contrast enhancement is correlated with microvascular density, histoprognostic factors and survival. Pancreatology. 2006;6(1–2):77–85.
8. d'Assignies G, Couvelard A, Bahrami S, Vullierme M-P, Hammel P, Hentic O, et al. Pancreatic Endocrine Tumors: Tumor Blood Flow Assessed with Perfusion CT Reflects Angiogenesis and Correlates with Prognostic Factors 1. Radiology [Internet]. 2009 Feb [cited 2019 May 20];250(2):407–16. Available from: http://www.ncbi.nlm.nih.gov/pubmed/19095784
9. Zamboni GA, Ambrosetti MC, Zivelonghi C, Lombardo F, Butturini G, Cingarlini S, et al. Solid non-functioning endocrine tumors of the pancreas: correlating computed tomography and pathology. HPB [Internet]. 2017 Nov [cited 2019 May 23];19(11):986–91. Available from: http://www.ncbi.nlm.nih.gov/pubmed/28784262
10. WHO Classification of Tumours of the Digestive System. Fourth Edition - WHO - OMS - [Internet]. [cited 2019 Jun 23]. Available from: http://apps.who.int/bookorders/anglais/detart1.jsp?codlan=1&codcol=70&codcch=4003&content=1
11. Choe J, Kim KW, Kim HJ, Kim DW, Kim KP, Hong SM, et al. What is new in the 2017 world health organization classification and 8th american joint committee on cancer staging system for pancreatic neuroendocrine neoplasms? Vol. 20, Korean Journal of Radiology. Korean Radiological Society; 2019. p. 5–17.
12. Youden WJ. Index for rating diagnostic tests. Cancer. 1950;3(1):32–5.
13. Sallinen V, Haglund C, Seppänen H. Outcomes of resected nonfunctional pancreatic neuroendocrine tumors: Do size and symptoms matter? Surg (United States). 2015 Dec 1;158(6):1556–63.
14. Partelli S, Cirocchi R, Crippa S, Cardinali L, Fendrich V, Bartsch DK, et al. Systematic review of active surveillance versus surgical management of asymptomatic small non-functioning pancreatic neuroendocrine neoplasms. Vol. 104, British Journal of Surgery. John Wiley and Sons Ltd; 2017. p. 34–41.
15. Rosenberg AM, Friedmann P, Del Rivero J, Libutti SK, Laird AM. Resection versus expectant management of small incidentally discovered nonfunctional pancreatic neuroendocrine tumors. In: Surgery (United States). Mosby Inc.; 2016. p. 302–10.
16. Worhunsky DJ, Krampitz GW, Poullos PD, Visser BC, Kunz PL, Fisher GA, et al. Pancreatic neuroendocrine tumours: hypoenhancement on arterial phase computed tomography predicts biological aggressiveness. HPB (Oxford) [Internet]. 2014 Apr [cited 2019 May 20];16(4):304–11. Available from: http://www.ncbi.nlm.nih.gov/pubmed/23991643
17. Gu D, Hu Y, Ding H, Wei J, Chen K, Liu H, et al. CT radiomics may predict the grade of pancreatic neuroendocrine tumors: a multicenter study. Eur Radiol. 2019 Dec 1;29(12):6880–90.
18. Canellas R, Burk KS, Parakh A, Sahani D V. Prediction of pancreatic neuroendocrine tumor grade based on CT features and texture analysis. Am J Roentgenol. 2018 Feb 1;210(2):341–6.
19. Takumi K, Fukukura Y, Higashi M, Ideue J, Umanodan T, Hakamada H, et al. Pancreatic neuroendocrine tumors: Correlation between the contrast-enhanced computed tomography features and the pathological tumor grade. Eur J Radiol [Internet]. 2015 Aug [cited 2019 May 20];84(8):1436–43. Available from: http://www.ncbi.nlm.nih.gov/pubmed/26022520